

Monitoring Masonry Walls Subjected to Earthquake Loading with a Time-of-Flight Range Camera

David HOLDENER, Dr. Derek D. LICHTI, Jeremy STEWARD, and Pedram KAHEH,
Canada

Key words: Photogrammetry, Range Camera, Loading Test, Civil Engineering Infrastructure

SUMMARY

Structural loading tests are usually observed with sensors capable of measuring only single point locations and in one dimension. Such sensors have to be placed close to or in contact with the moving object and are therefore at risk of damage in destructive experiments. The time-of-flight (ToF) range camera technology allows the collection of areal 3D measurements at video frame rate from a safe distance. This enables the monitoring of a complete structure with a single sensor. The requirement of only one relatively low-cost and compact active sensor is an additional advantage compared to passive imaging approaches that require at least two sensors or terrestrial laser scanners that cannot image dynamic scenes. This paper presents a ToF range camera approach to measure the structural deformations of masonry walls of size 2.2 x 2.2 x 0.2 m subjected to earthquake loading on a single-axis shake table. The loading tests were performed with the walls placed parallel to the direction of motion for in-plane movement (three tests) and orthogonal to direction of motion for out-of-plane movement (two tests). The dynamic experiments as well as static observations were conducted with a SwissRanger SR4000 range camera and signalized targets attached to the walls.

Based on these measurements, the potential and limitations of such sensors are evaluated in terms of precision and temporal resolution for dynamic structural loading tests. Static tests to quantify the precision show a high dependence on the radial distance in the image plane. Central targets in single frames could be measured with an RMS of 0.4 mm in position (X, Y) and 5 mm in range (Z), whereas at the periphery of the image format, the precision decreased to an RMS of 7 mm (position) and 18 mm (range). To detect the smallest deformations possible, the measurements were averaged temporally with a moving average over five camera frames. This improved the precision in range to 2 mm - 8 mm and in position below 3.5 mm. Comparison of the in-plane movement measured from the SR4000 with a laser displacement sensor quantified the tracking precision per frame up to 1.3 mm RMS. The results show that the range camera can bring additional information for the analysis of structural loading tests.

Monitoring Masonry Walls Subjected to Earthquake Loading with a Time-of-Flight Range Camera

David HOLDENER, Dr. Derek D. LICHTI, Jeremy STEWARD, and Pedram KAHEH,
Canada

1. INTRODUCTION

Earthquakes have high damage potential for buildings and infrastructure. Especially masonry walls often do not show a ductile behaviour due to a lack of reinforcement or poor maintenance and are more prone to damage than strengthened walls during an earthquake. Therefore, it is necessary to strengthen existing masonry structures in areas with high seismicity. A collaborative research between the Universities of British Columbia, Calgary and Manitoba has the goal to improve the behaviour of existing masonry structures such as schools and office complexes in British Columbia, Canada, to reduce the risk of collapsing during a seismic event by applying an Eco-friendly Ductile Cementitious Composite (EDCC) repair material. Previous structural experiments comparing reinforced and non-reinforced hollow concrete masonry walls already showed an increasing stiffness, ductility and drift capacity for the in-plane behaviour (Kaheh et al., 2016) as well as changing characteristics during free vibration tests (Kaheh & Shrive, 2016). The latest conducted experiments described in this report aim to assess the dynamic behaviour of the repair material on walls placed on a shake table in a structural testing laboratory. Such laboratory experiments are important to validate designs before applying them in larger scale outside the safe testing environment.

Conventional techniques for deformation monitoring in structural engineering experiments include, for example, wire grid gauges, fibre-optic sensors, accelerometers and laser displacement sensors. They are usually high-precision tools and can measure at high temporal frequency. Since these sensors are all contact based or have a limited range, they have to be placed on or very close to the specimen tested. In case of a failing structure, the instruments are at risk of being damaged. An additional drawback is the limitation to collect only point-based measurements, usually only in one dimension, which makes it infeasible to configure multiple sensors in order to achieve areal coverage for the entire specimen. Detchev (2016) lists the desirable characteristics of a laboratory infrastructure monitoring system as the following:

- Non-contact to avoid damage
- Ability to observe both static and dynamic scenes
- Based on low-cost, off-the-shelf components
- Capable of 3D reconstruction of entire homogeneous objects
- Precise measurements of the needed parameters
- High level of automation

This paper reports on tests of the applicability of the SR4000 time-of-flight range camera for structural loading tests in the described experiments. As this is an active imaging technique, the sensor is non-contact and can cover homogeneous surfaces, without the need of targets, in three dimensions. In comparison to image based approaches using photogrammetry, the range camera needs only one sensor and is therefore easy to handle and not reliant on object texture. The camera is able to cover whole objects with video frame rate which is not possible for terrestrial laser scanners. However, major drawbacks of this system are the limited precision, measurement frequency and resolution as well as some scene dependent errors. After a brief description of the measurement principle and range camera error sources, the experimental setup is described followed by the achievable results regarding the precision and the utility.

2. RANGE IMAGING

Range cameras like the SwissRanger SR4000 used in this work are based upon continuous-wave modulation and phase shift measurements as described in Lange & Seitz (2001) to determine ranges by the ToF principle. A set of integrated light emitting diodes (LEDs) illuminates the scene with modulated light in the near infrared (NIR) portion of the spectrum. The light reflected back from objects in the scene is focused onto the CCD-array of the camera. To calculate the phase difference, four phase signals with a 90° phase delay are sent out after each other. After a pre-defined integration time, the phase measurement is determined for each signal, from which the phase difference and the geometric distance are then determined. The result is a range and intensity measurement for each pixel. The final output of the range camera is a collocated 3D point cloud and an amplitude image.

A classification of the random and systematic error sources into four groups is shown by Lichti & Kim (2011). The first group are the random errors due to the measurement process of the photons by the range camera. The source and influence of the so-called shot and dark noise is described in Lange & Seitz (2001). Scene-dependent systematic errors are the second group and occur due to the measurement environment or the structure of the scene. In laboratory conditions, environmental influences like the temperature can be kept under control, whereas for measurements outside the laboratory such errors have to be accepted. The scene layout can lead to multipath if one pixel measures both fore- and background due to the finite resolution. Internal light scattering can occur if the scene has a bright foreground. In this situation, light returned from a bright foreground experiences multiple reflections inside the camera and causes a range bias to the surrounding background (Mure-Dubois & Hügli, 2007). Errors due to the warm-up and integration time are the third group of error sources. To minimize the influence of these camera operating parameters, Piatti & Rinaudo (2012) recommend a warm-up time of at least 40 minutes and to keep the integration time during the whole data acquisition constant. The fourth group are systematic instrumental errors from camera components or their assembly such as lens distortions and ranging errors. These errors can usually be modelled and calibrated prior to the data acquisition. In addition to these error sources, Hansard et al. (2013) report motion blur. This occurs when either the camera or the object in the scene is in motion. The camera assumes a static scene during the integration time of the four phase signals for one frame. If there is motion during the integration time and with this during the

depth calculation, this measurement will be corrupted. In contrast to pre-processing methods to compensate motion artefacts, Qi & Lichti (2012) set up an experiment to determine the best frame rate under a given periodic motion frequency and amplitude. For a 4 mm / 3 Hz motion this resulted in a minimal frame rate requirement of 20 Hz to keep the error in an acceptable range.

3. EXPERIMENT SETUP

3.1 Camera Specifications

For the experiments conducted in this work, the wide angle version of the SwissRanger SR4000 ToF camera was used. An overview with the most important specifications is given in Table 1:

Table 1: Specification of the SwissRanger SR4000 wide angle version (MESA Imaging, 2011)

Specification	Value
Pixel resolution	176 x 144
Pixel pitch	40 μm
Maximal frame rate	50 FPS
Calibrated depth range	0.8 – 5.0 m
Field of view	69° x 56°
Focal length	5.8 mm
Absolute accuracy	± 10 mm
Repeatability of central pixels (1σ)	4 - 7 mm

The manufacturer (MESA Imaging, 2011) specifies the distance measurement accuracy as ± 10 mm and the repeatability as 4 - 7 mm (1σ). This repeatability is given for central pixels and can increase by factor 2 for pixels at the periphery of the image format. Experimental tests have proven these specifications (e.g. Chiabrando et al., 2010). The data outputs of the SR4000 are the range and amplitude values (16 bit) in images as well as the 3D point cloud in the local Cartesian camera coordinate system. In addition, the camera provides a confidence map with the quality of the measured data.

3.2 Design of Experiment

The stability of several masonry walls—some with strengthening material applied—was tested during simulated earthquakes on a shake table. The shake table is capable of performing one-dimensional movement with a maximum amplitude of ± 15 cm from the initial position. The input signals for the shake table were measurements from real earthquakes and artificial sinusoidal curves with frequencies between 0.1 - 25 Hz. The walls had the dimensions of 2.2 x 2.2 x 0.2 m with a brick size of 38 x 19 x 19 cm. The targets on the wall had to be smaller than the bricks to prevent covering the mortar between the bricks where the first cracks will usually appear. The chosen 150 mm target size was the largest possible that would fit on a single brick and still allow a robust extraction from the amplitude imagery.

The acquisition time of the camera was set to achieve a 30 Hz measurement frequency. A higher frequency over 50 Hz would be preferable to cover the whole range up to 25 Hz of the input signal. However, the maximal frame-rate of the SR4000 is at 50 Hz and more frames per second result in a lower signal to noise ratio due to the shorter integration time. Thirty FPS was therefore chosen as a good trade-off between frame rate, level of noise and motion blur (Qi et al., 2014). The same camera was used for all experiments. A total of five walls were tested: three of them under lateral movement and two under orthogonal movement. An overview of the conducted experiments is given in Table 2 and of the different input signals in Table 3.

Table 2: Overview wall experiments

Wall No.	Movement	Repair material	Signals (Table 3)
1	lateral	reinforced	1, 2
2	lateral	reinforced	1 - 4
3	lateral	reinforced	1 - 4
4	orthogonal	non-reinforced	1 (only 25%)
5	orthogonal	non-reinforced	1 (only 25%)

Table 3: Overview input signals

No.	Name	Source	Duration [s]	Magnitude [%]
1	Kobe	recording	41	25, 50, 75, 100, 125
2	Tohoku	modified	109	50, 75, 100, 125
3	Northridge	recording	40	75, 100, 130
4	Sinusoidal	artificial	~ 45	100

3.2.1 Lateral Movement

For the experiments with the lateral movements, the range camera was mounted on a steel beam in a tilted position with a distance of 2.75 m from the wall and 4 m to the background (Figure 1). The camera was oriented such that the optical axis was directed to the centre of the wall with an orthogonal incidence angle. The camera was rolled by 90° to align the long dimension of the image format with the vertical dimension of the wall. Since the space in the laboratory and the maximum range of the camera are limited, either a good horizontal or vertical coverage was possible. The interesting deformations in the wall are expected to be between the lower and the higher parts of the wall. Therefore, it is more important to cover all rows of targets, whereas it was not a big problem if a column of targets is missing.

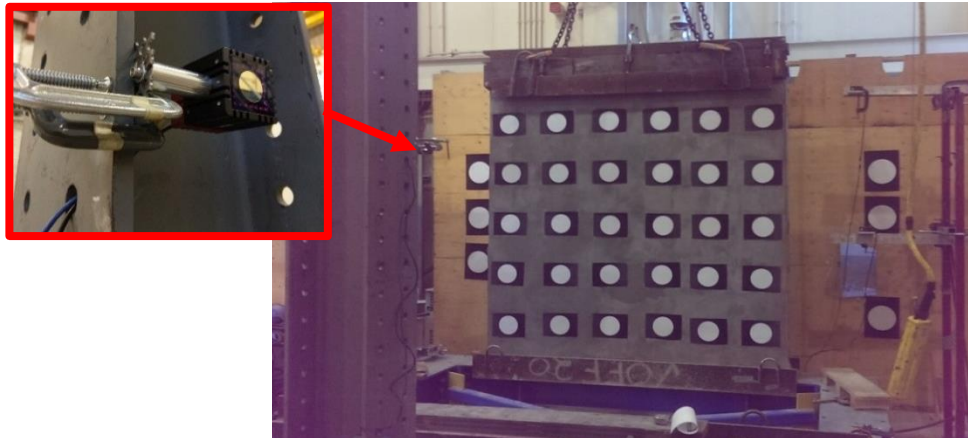


Figure 1: Experiment setup for tests with lateral movement

Three walls with applied strengthening material were tested under lateral movement. The experiment with the first wall was only conducted with the input signals 1 and 2. Due to the small deformations, the later experiments were performed with all four input signals. The different signals were all tested after each other with increasing magnitude from 25% of the observed earthquake up to 130%. The sinusoidal signal 4 led to failure of both walls near their base. Even though the same reinforcement material was used for all specimens, different behavior and deformations were observed during the loading tests.

3.2.2 Orthogonal Movement

The range camera was mounted on the same beam in a tilted position for the experiments with the orthogonal movement as for the lateral one. The camera had an incidence angle to the wall of approximately 45° due to the arrangement of the wall on the shake table and the presence of additional steel beams for safety reasons (Figure 2). The distance between the wall and the camera was between 1.5 m and 2.5 m. During this project, only two plain masonry walls without repair material were tested under orthogonal loading. Each wall was only tested with input signal 1 (Kobe) and a signal strength of 25% of the real observed earthquake. Both walls failed at this level of magnitude.

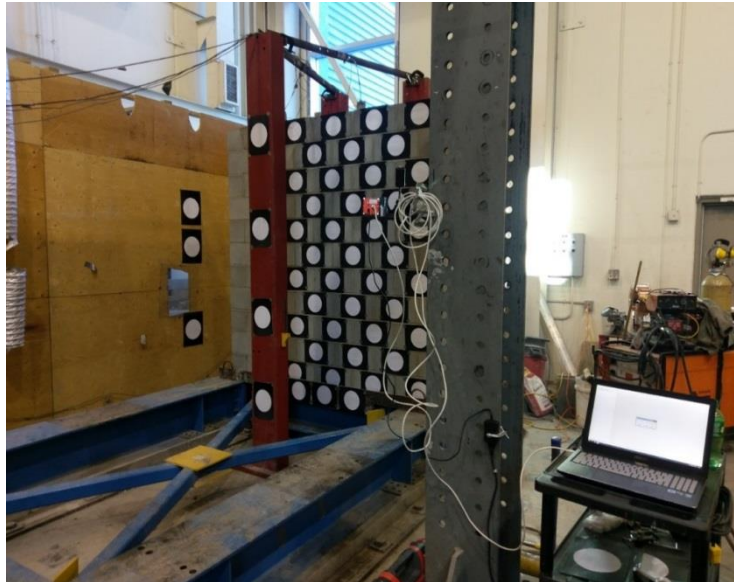


Figure 2: Experiment setup for tests with orthogonal movement

3.2.3 Additional Sensors

All the experiments were also measured with the conventional sensors. Three laser displacement sensors (LDS) were installed in the direction of the movement and at three different heights (at the bottom, middle and top of the wall). At the top and bottom of the wall, accelerometers were likewise installed. Each of these sensors can measure with a frequency of 2000 Hz. The LDS has a resolution of $1 \mu\text{m}$ and the accelerometer of $1 \mu\text{m/s}^2$. In addition to these measurements, the shake table's input signal was also available for comparisons and verification of the camera. The input signals 1 and 3 are computed with a frequency of 100 Hz and input signal 2 with 256 Hz.

3.3 Data Processing

The targets placed on the wall were tracked in the SR4000 amplitude image time series using a least squares ellipse fit. The 3D coordinates were computed using these image space coordinates and the range measurement. To obtain a set of meaningful coordinates, they were transformed into a system defined by the zero state targets of the wall on the shake table (Figure 3). The X-axis was defined to coincide with the vertical movement or deformation direction, the Y-axis for lateral shifts and the Z-axis for orthogonal movement in the horizontal plane. In a first step, the Z-axis was defined by the normal of a plane fit including all target points on the wall. The Y-axis was then computed using a line fit through the bottom row targets and constrained to be orthogonal to the Z-

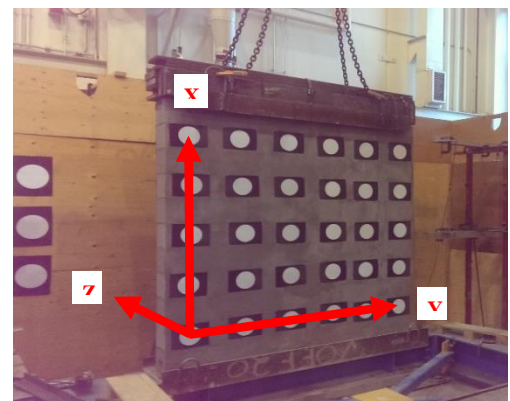


Figure 3: Definition of the coordinate system by the wall in zero state position

axis. The X axis was constrained to be orthogonal to Y and Z without any target measurements. The definition of these axes resulted in the rotation matrix for the transformation. The translation was performed to define the origin of the coordinate system at the bottom left target.

4. EXPERIMENTAL RESULTS

4.1 Static Repeatability

Two static datasets of 45 seconds (1350 frames) were captured with the SR4000 directly after each other to quantify the repeatability of the experiments. Data from the first 30 seconds (900 frames) of the first observation series were averaged to use as the zero load state reference for the dynamic experiments. The RMS was computed for every target point based on this time series. Because the precision is highly dependent on the radial distance in the image plane, the minimal, maximal and mean RMS are used for the evaluation. The raw observations are the image space coordinates (x and y) from the ellipse fit to the targets, in pixels, and the range value (ρ) from the range image at the determined image coordinates, in mm. The results are presented in Table 4:

Table 4: Static repeatability (RMS) of raw measurements and 3D coordinates

		Minimal RMS	Maximal RMS	Mean RMS
Raw measurements	x [px]	0.002	0.096	0.031
	y [px]	0.002	0.079	0.031
	ρ [mm]	5.4	20.2	10.3
3D coordinates	X [mm]	0.1	7.3	2.4
	Y [mm]	0.4	7.0	2.5
	Z [mm]	5.4	17.6	9.7

For the 3D object space coordinates, the range measurements are the main source of error in all three directions due to the error propagation. Figure 4 shows the RMS values in object space for each target. Z is mainly dependent on the radial distance and X & Y increase with their distance in X / Y from the image centre.

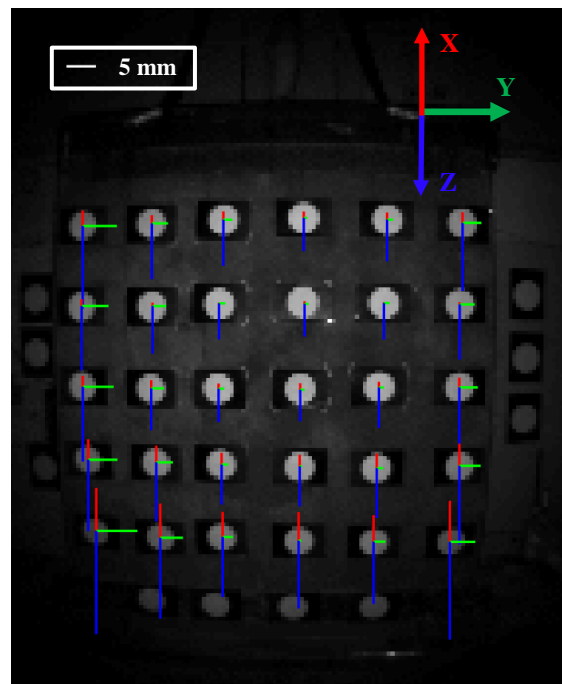


Figure 4: Distribution of object space RMS values

A simple way to improve the repeatability is averaging. This was done in object space with the final 3D coordinates either by averaging multiple targets or with a moving average over multiple frames. By applying a moving average, the level of noise reduces and the time series is easier to interpret and trends or signals are clearer. A drawback of this kind of averaging is that measured peaks in the time series to be detected are flattened. An averaging window size of five values gave the best results regarding the elimination of noise and being able to detect important features in the time series. Multiple targets in a single frame can be averaged and represent the movement or deformation of a larger part of the wall if a rigid body can be assumed due to knowledge about the specimen. Such an assumption of a rigid body should not be made in general but can deliver additional information for particular experiments and motions. For this experiment, the averaging of all targets in a column and the averaging over all rows of targets was tested. Especially the later dataset provided a deeper insight regarding the deformation of the specimen. It is also possible to combine both averaging methods to eliminate the noise even more and make the data better interpretable. RMS values below 3 mm for averaged targets with a large radial distance can be achieved. The detailed results are listed in Table 5.

So far, the coordinates have only been compared regarding their absolute movement to the zero state. For a deeper analysis of the wall deformation, relative movement between two targets can be

computed. The main drawback however is the decreasing precision as it is added up from both targets used for the relative comparison.

Table 5: Static repeatability (RMS) of single and averaged point coordinate (3D) [mm]

	Minimal RMS	Maximal RMS	Mean RMS
Single targets	5.4	20.3	10.3
Moving average of 5	2.4	9.1	4.6
Averaged row (6 targets)	3.5	6.6	4.6
Averaged row & moving average of 5	1.7	2.9	2.0

4.2 Dynamic Comparison with other Sensors

To verify the datasets captured with the range camera in dynamic experiments, they were compared to the theoretical input signal and the LDS data. The resulting one-dimensional differences are highly dependent on the selected target and the input signal as targets have different levels of noise depending on their radial distance and signals with high frequencies are more difficult to capture by the camera. The best RMS values could be achieved using a central target and comparing the measurement from the Kobe signal with the lowest magnitude (25%). The difference between camera observations and input signal as well as the comparison with the LDS have a RMS of 1.3 mm. The time series with the measurements from the SR4000 and the LDS are shown in Figure 5. The differences can increase even with a central target up to 2.7 mm for signals with higher frequencies like Tohoku at 125% magnitude.

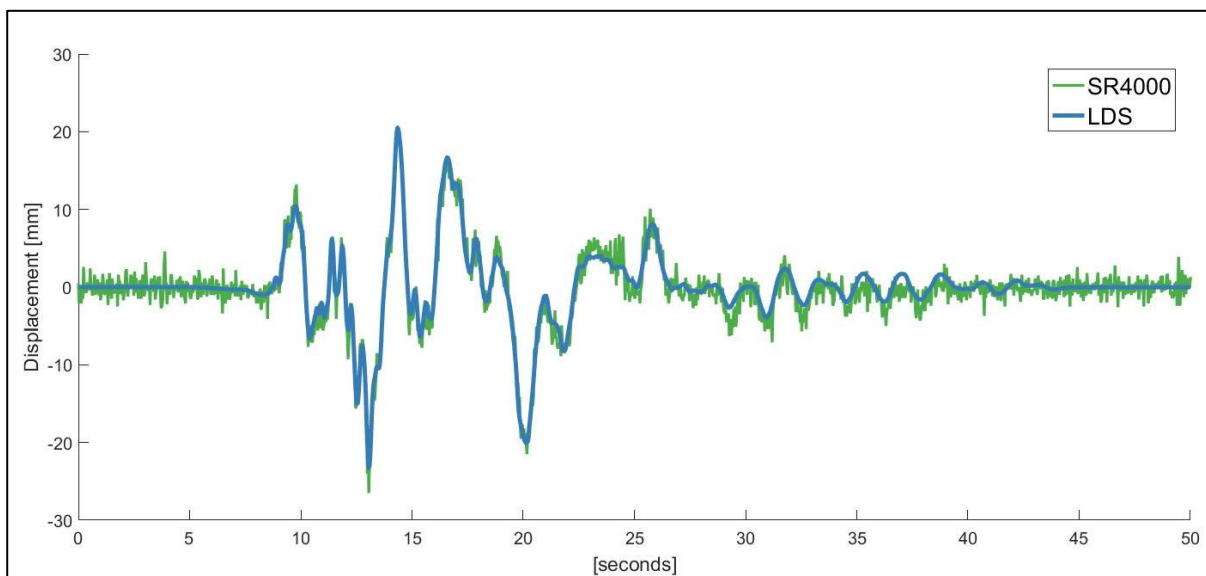


Figure 5: Displacement measured by the SR4000 range camera (central target without averaging) and the LDS with input signal 1 (Kobe) at 25% magnitude

4.3 Time Series Analysis

An easy way to visualize and analyse the observations is in a time series. As the coordinates are defined by the wall, they are already describing the movement and deformation occurred (Figure 3). Two examples of the resulting time series are discussed in this paper: Figure 6 presents a lateral wall setup with a sinusoidal input signal where the movement of the wall was in the Y direction and the main deformation was in Z. An orthogonal setup is shown in Figure 7 with the Kobe input signal at 25% magnitude. The movement of the wall and its deformation both occur in Z direction in this case.

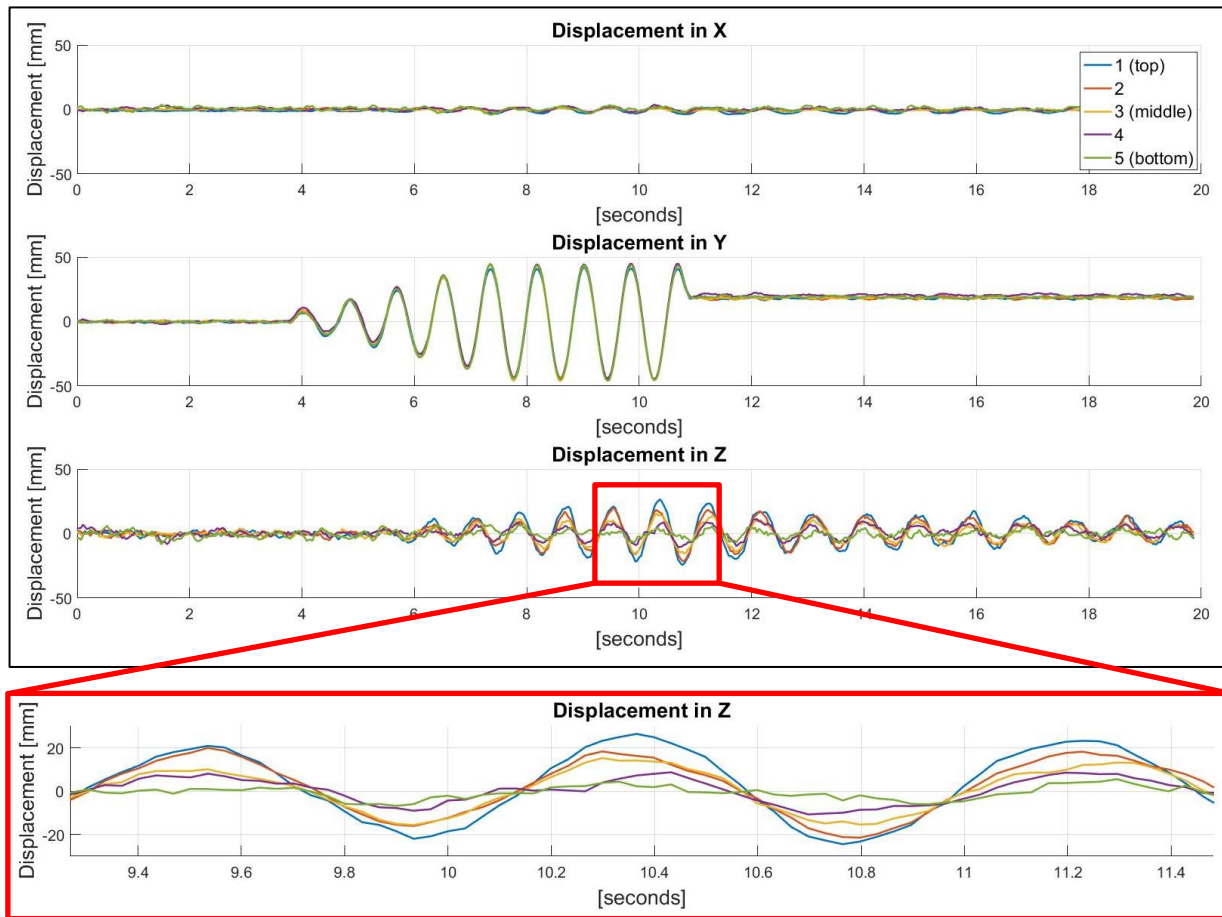


Figure 6: Time series of wall 3 (lateral setup) with sinusoidal input signal (No. 4) manually stopped after 11 seconds, averaged per row and moving average of 5

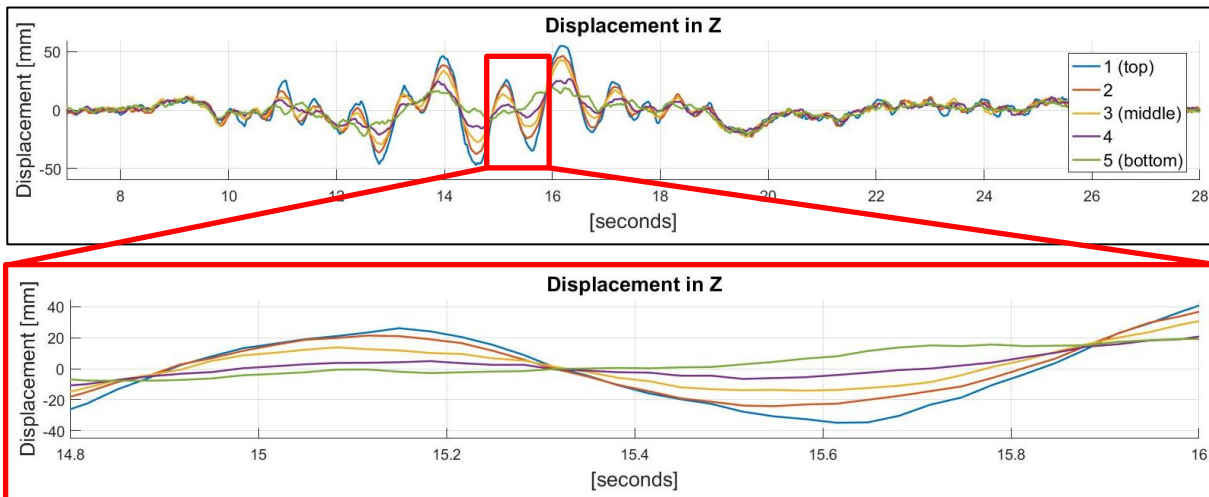


Figure 7: Time series of wall 5 (orthogonal setup) with input signal 1 (Kobe) at 25% magnitude, averaged per row and moving average of 5

As it can be expected, the deformation in the top row is the largest with up to 25 mm and decreases toward the base of the wall. Another valuable quantity that can be read from this data is the delay of the maximal amplitude in case of the orthogonal movement. A good example for this can be seen in Figure 7, where the peaks of the maximal amplitude are delayed for top row targets. This suggests that the top targets move more independently from the shake table and there is some failure between the bricks.

In addition to the time series, the results can be transformed to the Fourier space to gather more information about the wall's behaviour. Figure 8 presents an example from a lateral setup with the input signal 1 and 100% magnitude. The observations from the range cameras are compared to the input signal and the LDS measurements. The spectra all match very well in terms of the frequency locations of the peaks. Overall, the magnitudes of the measurement spectra are slightly lower than that of the input signal, which likely indicates that the hydraulic presses do not transfer the theoretical input completely to the shake table, there are frictional losses and/or that there are losses between shake table and wall specimen.

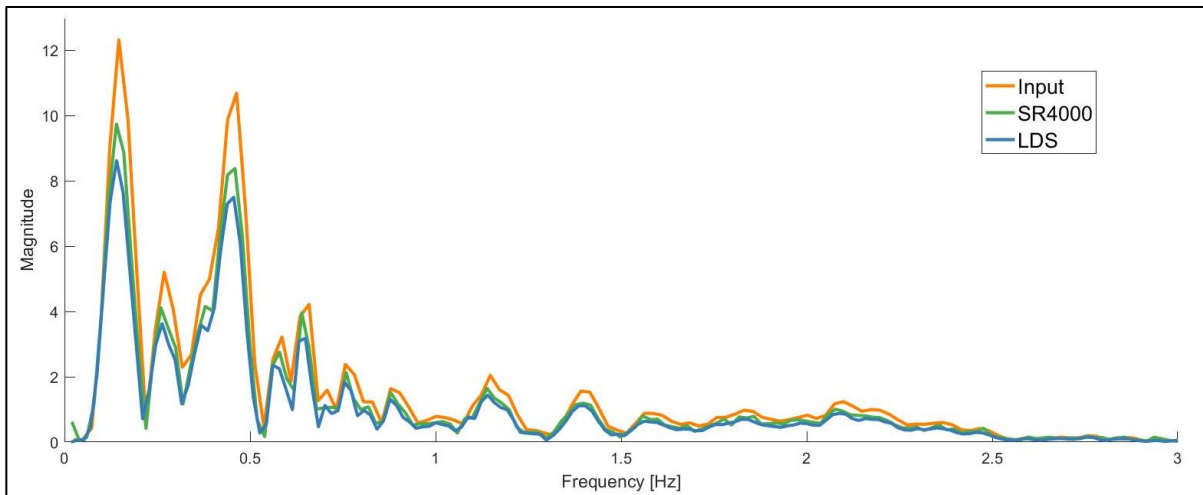


Figure 8: Fourier space analysis of wall 1 (lateral setup) with input signal 1 (Kobe) at 100% magnitude

5. CONCLUSION

Structural loading tests have successfully been observed using the SR4000 time-of-flight range camera and targets mounted to the specimen. Static tests show a high dependency of the precision of the measurements on the radial distance in the image plane. Thanks to a temporal moving average, the precision of all points improve to RMS values of 9 mm or smaller for the 3D coordinates. The assumption of a rigid body can only be made in special cases but allows the averaging of multiple targets in a single frame to improve the precision further. The comparison between the processed range camera data and the input signal or the laser displacement sensor reveal a concordance with RMS values of 1.3 – 2.7 mm. These evaluations show the limitation of the range imaging technology regarding the precision and also the measurement frequency is not as high as it should be to cover the whole signal of an earthquake. However, also the advantages of the range camera could be utilised to gain additional insight into the dynamic behavior of the captured walls. This is particularly the areal coverage of three dimensional data which delivered additional information compared to the traditional sensors in use.

A deeper analysis of the results regarding the effectiveness of the repair material was not possible as there were no measurements of a reinforced and a non-reinforced wall with the same configuration so far. Further, the extraction of continuative information about the deformation or the observation without targets is still open for further research.

ACKNOWLEDGMENTS

Support for this project was provided by the Natural Sciences and Engineering Research Council (NSERC) of Canada, the Canada Foundation for Innovation and BrXton. The Alberta Masonry Council, the Masonry Contractors Association of Alberta (South) and the Canadian Concrete

Masonry Producers Association are thanked for their help with building the specimens. The support of the technical staff of the Department of Civil Engineering at the University of Calgary is much appreciated.

REFERENCES

- Chiabrando, F., Piatti, D. & Rinaudo, F. (2010). SR-4000 ToF camera: further experimental tests and first applications to metric surveys. *International Archives of Photogrammetry, Remote Sensing and Spatial Information Sciences*, 38(5), pp.149–154.
- Detchev, I. (2016). *Image-based Fine-scale Infrastructure Monitoring*. Dissertation. University of Calgary.
- Hansard, M., Lee, S., Choi, O. & Horaud, R. (2013). *Time-of-Flight Cameras: Principles, Methods and Applications*. Berlin: Springer.
- Kaheh, P. & Shrive, N. (2016). Effects of eco-friendly ductile cementitious composites (EDCC) on dynamic characteristics of hollow concrete masonry walls. *Brick and Block Masonry – Trends, Innovations and Challenges*. 16th International Brick and Block Masonry Conference. Padova: Taylor & Francis Group, pp.2109–2116.
- Kaheh, P., Shrive, N., Soleimani-Dashtaki, S. & Banthia, N. (2016). Influence of eco-friendly ductile cementitious composites (EDCC) on in-plane behaviour of hollow concrete masonry walls. *Brick and Block Masonry – Trends, Innovations and Challenges*. 16th International Brick and Block Masonry Conference. Padova: Taylor & Francis Group, pp.2117–2125.
- Lange, R. & Seitz, P. (2001). Solid-State Time-of-Flight Range Camera. *IEEE Journal of Quantum Electronics*, 37(3), pp.390–397.
- Lichti, D. & Kim, C. (2011). A comparison of three geometric self-calibration methods for range cameras. *Remote Sensing*, 3(5), pp.1014–1028.
- MESA Imaging (2011). SR4000 Data Sheet. Available at: <http://www.adept.net.au/cameras/Mesa/pdf/SR4000.pdf> [Accessed 8 Sep. 2016].
- Mure-Dubois, J. & Hügli, H. (2007). Optimized scattering compensation for time-of-flight camera. *Optics East*. International Society for Optics and Photonics. Bellingham
- Piatti, D. & Rinaudo, F. (2012). SR-4000 and CamCube3.0 Time of Flight (ToF) Cameras: Tests and Comparison. *Remote Sensing*, 4(4), pp.1069–1089.
- Qi, X. & Lichti, D. (2012). Dynamic concrete beam deformation measurement with 3D range cameras. *International Archives of Photogrammetry, Remote Sensing and Spatial Information Sciences*, 39(B5), pp.239–244.
- Qi, X., Lichti, D., El-Badry, M., Chan, T.O., El-Halawany, S.I., Lahamy, H. and Steward, J. (2014). Structural dynamic deflection measurement with range cameras. *The Photogrammetric Record*, 29(145), pp.89–107.

BIOGRAPHICAL NOTES

David Holdener is currently studying for his Master of Science in Engineering with a specialisation in Geoinformation Technology at the FHNW University of Applied Sciences and Arts

Northwestern Switzerland. He completed his undergraduate studies at the same institution in Geomatics Engineering. In both his undergraduate and graduate studies, he was working on different research projects in the field of imaging metrology.

Dr. Derek Lichti is currently Professor and Head of the Department of Geomatics Engineering at the University of Calgary and Editor-in-Chief of the ISPRS Journal of Photogrammetry and Remote Sensing. His research program is focused on developing solutions for the exploitation of optical and range-imaging sensors for the automated creation of accurate 3D models for measuring human motion, monitoring structural deformation and compiling asset inventories of the built environment.

CONTACTS

Mr. David Holdener
FHNW University of Applied Sciences and Arts Northwestern Switzerland
Institute of Geomatics Engineering
Gründenstrasse 40
4132 Muttenz
SWITZERLAND
Email: david.holdener@students.fhnw.ch

Prof. Derek Lichti
University of Calgary
Department of Geomatics Engineering
2500 University Drive NW
Calgary AB T2N 1N4
CANADA
Tel. +1 403 210 9495
Fax +1 403 284 1980
Email: ddlichti@ucalgary.ca
Web site: <http://www.ucalgary.ca/lichti/>

Mr. Jeremy Steward
University of Calgary
Department of Geomatics Engineering
2500 University Drive NW
Calgary AB T2N 1N4
CANADA
Email: stewardj@ucalgary.ca

Mr. Pedram Kaheh
University of Calgary
Department of Civil Engineering
2500 University Drive NW

Monitoring Masonry Walls Subjected to Earthquake Loading with a Time-of-Flight Range Camera (9073)
David Holdener (Switzerland), Derek D. Lichti, Jeremy Steward and Pedram Kaheh (Canada)

FIG Working Week 2017
Surveying the world of tomorrow - From digitalisation to augmented reality
Helsinki, Finland, May 29–June 2, 2017

Calgary AB T2N 1N4
CANADA
Email: pkaheh@ucalgary.ca

Monitoring Masonry Walls Subjected to Earthquake Loading with a Time-of-Flight Range Camera (9073)
David Holdener (Switzerland), Derek D. Lichti, Jeremy Steward and Pedram Kaheh (Canada)

FIG Working Week 2017
Surveying the world of tomorrow - From digitalisation to augmented reality
Helsinki, Finland, May 29–June 2, 2017